Oceanologia (2017) 59, 422—430

Available online at www.sciencedirect.com

ScienceDirect

journal homepage: www.journals.elsevier.com/oceanologia/

ORIGINAL RESEARCH ARTICLE

Aerosol Optical Depth variations due to local breeze circulation in Kongsfjorden, Spitsbergen

Malgorzata Cisek*, Tomasz Petelski, Tymon Zielinski, Przemyslaw Makuch, Paulina Pakszys, Anna Rozwadowska, Piotr Markuszewski

Institute of Oceanology, Polish Academy of Sciences, Poland

Received 9 July 2016; accepted 6 April 2017
Available online 24 May 2017

KEYWORDS
Aerosol Optical Depth;
Regional aerosol modifications;
Breeze circulation;
Svalbard

Summary This paper presents the results of Aerosol Optical Depth (AOD) studies which took place in Ny-Ålesund in the spring of 2014 during the iAREA campaign. The measurements were taken using Microtops II hand-held sunphotometers along the Kongsfjorden, on a path leading from the research village to the fjord opening. Local breeze circulation was observed during the measurement campaign which resulted in an evident increase of AOD along the measurement profile towards the open sea. Using the observed AOD, changes over the open sea have been calculated and the location of the breeze front has been determined.

1. Introduction

Aerosol optical properties vary in space and time, and it is especially noticeable in the Arctic. Higher values of Aerosol Optical Depth (AOD) in the spring — the Arctic haze season — and lower values during the summer months have been reported by scientists from various stations around the Arctic region (Tomasi et al., 2007, 2015). The range of AOD deviation at 500 nm varies from 0.12 to over 0.35 (Arctic haze conditions), to values not exceeding 0.1 or even less than 0.05 (clean summer conditions) (Stone et al., 2014; Tomasi et al., 2007). Such a seasonal dependency of AOD values is a result of a wide range of aerosol loads, their composition and size distribution (Herber et al., 2002; Tomasi et al., 2007, 2015) which causes the seasonal chemical composition and the particle size distribution of aerosols to differ considerably. Later into the winter and spring seasons, aged accumulation-mode particles play a dominant role in the number distribution of submicron particles in Spitsbergen. However, in the summer, small particles (Aitken-mode) are prevailing in the Arctic air (Engvall et al., 2008). In the summer, sulfate and sea salt aerosols contribute most to submicron light scattering, while supermicron particle scattering is usually

* Corresponding author at: Institute of Oceanology, Polish Academy of Sciences, Powstańców Warszawy 55, 81-712 Sopot, Poland. Tel.: (+48 58) 73 11 821; fax: (+48 58) 551 21 30.
E-mail address: gosiak@iopan.gda.pl (M. Cisek).
Peer review under the responsibility of Institute of Oceanology of the Polish Academy of Sciences.

Production and hosting by Elsevier

http://dx.doi.org/10.1016/j.oceano.2017.04.005

dominated by sea salt. This phenomenon is most significant in the summer due to broken sea ice (Quinn et al., 2007; Tomasi et al., 2007).

In mesoscale, the advection of anthropogenic aerosols, biomass burning, dust and volcanic aerosols from lower latitudes is significant and has a strong impact on the aerosol load in the Arctic (Generoso et al., 2007; Hirdman et al., 2010; Law and Stohl, 2007; Stohl, 2006; Tomasi et al., 2007, 2015; Treffeisen et al., 2011). In the winter and spring, conditions are best for long-range transport of aerosols and their gaseous precursors. This is due to the southward shift of the polar front, which facilitates the advection of polluted air from mid-latitudes (mainly from Europe and Asia). The effectiveness of the transport of aerosols and their gaseous precursors is additionally enhanced by a stable atmosphere and relatively low scavenging by clouds and precipitation (Quinn et al., 2007).

A potential effect of the increased concentrations of greenhouse gases in the atmosphere is manifested in the 0.6°C rise of the global mean surface temperature since the late 19th century (Nicholls et al., 1996). On a regional scale, the effects such a temperature increase has on precipitation, winds, cloud cover, etc. are not easy to describe (Gjelten et al., 2016), however, the majority of global circulation models show a poleward amplification of climate signals. Such changes result in a warming climate, which may be manifested in the polar regions, through a significant increase in climate variability and increasingly extreme weather situations, deeper cyclones, stronger seasonal cycles and higher precipitation. Until not long ago, no significant surface temperature trends have been observed in Svalbard, while the precipitation level has increased by as much as 25% since the beginning of the XX century (Førland et al., 1997). However, Maturilli et al. (2013, 2015) proved a decadal trend in surface temperature on a level of 1.35°K and 1.3°K.

On a smaller, spatial scale, measurements of wind speed and direction in the Arctic are rarely representative for larger areas surrounding the measurement stations. Many research stations in the Svalbard region have their own, locally typical wind regimes (Mazzola et al., 2012; Rozwadowska et al., 2010; Tomasi et al., 2007). One of the most important issues in the Svalbard fjords is the effect of local orography, which is often manifested by the wind channelling along the fjord axis (Argentini et al., 2003; Beine et al., 2001; Førland et al., 1997; Hanssen-Bauer et al., 1990; Hartmann et al., 1999). Hanssen-Bauer et al. (1990) reported that wind directions along the fjord axis dominate at all Svalbard stations. Additionally, other types of winds such as fens and downfall winds as well as local circulations of the breeze type are observed and they result from horizontal nonuniformity of temperature.

The climatology studies of the Ny-Ålesund and Kongsfjorden areas carried out by Esau and Repina (2012), Hanssen-Bauer et al. (1990) and Maturilli et al. (2013) confirm that for Kongsfjorden, surface winds usually blow along the axis of the fjord. Other types of winds, such as fen and katabatic winds also influence local wind climatology. However, Esau and Repina (2012), using an eddy-resolving model, proved that thermal land-sea breeze circulation is more significant than katabatic winds in Ny-Ålesund (Kongsfjorden). The same was reported by Cisek et al. (unpublished data). They also observed that this effect is true for the entire archipelago, including Hornsund in the south.

2. Study description

The studies were carried out in the area of Kongsfjorden and in Ny-Ålesund itself during the iAREA 2014 (Impact of Absorbing Aerosols on radiating forcing in the European Arctic (iAREA)) campaign which took place in Svalbard between 15 March and 4 May 2014. The iAREA project (http://www.igf.fuw.edu.pl/iAREA) is a part of the Polish-Norwegian Research Programme, and has been realized between 2013 and 2016. For the purpose of this paper, the authors present data from the measurements taken on 6 April 2014 only (Fig. 1).

On 6 April 2014 observations started at 8:55 UTC near the Alfred Wegener Institute (AWI) laboratory in the research

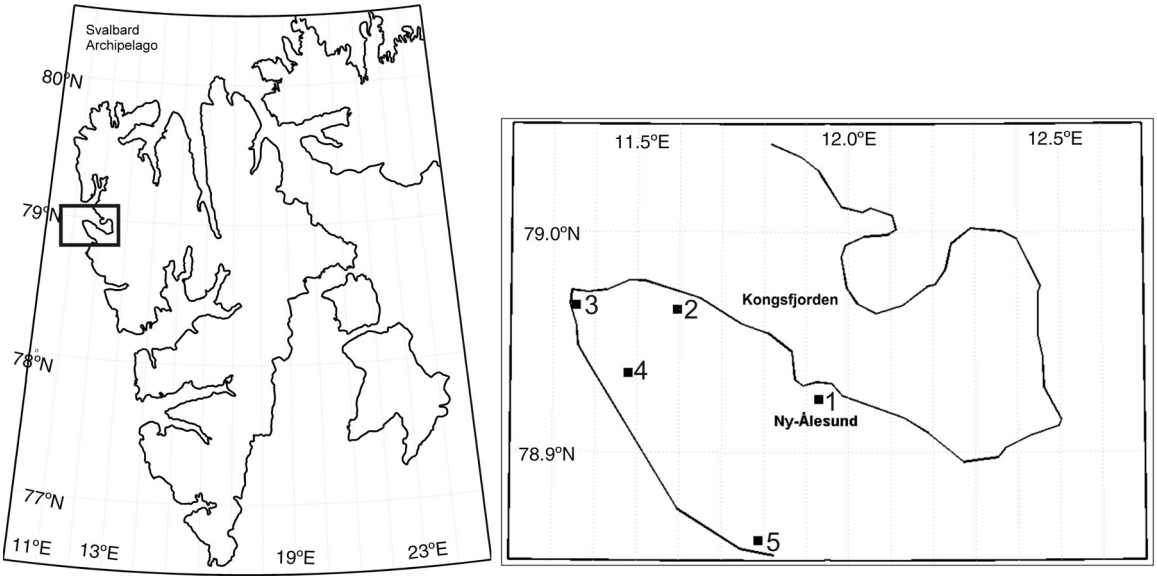

Figure 1 Location of the study area and measurement points in the Kongsfjorden.

village (78.92N, 11.92E). Data collection continued in that location until 10:30 UTC. Then, using a snowmobile, the research team moved north-west along the fjord. Measurements were also taken during relocation. Observations at the fjord opening (78.96N, 11.33E) started at 12:00 and lasted until 12:27 UTC. The subsequent observations were made on the outer side of the fjord, on the other side of the mountains. The very last two measurements were taken in the fjord again at 13:43 UTC. The rationale for such a measurement regime was to prove that breeze circulation is observed in the area and that it has an impact on local AOD levels.

The measurements were taken with two Microtops II sunphotometers (instruments No. 14475 and 15613). The Microtops II sunphotometer (produced by Solar Light Company USA) is a hand-held instrument for measuring Aerosol Optical Depth, water vapor column and direct irradiance at all selected wavelengths. The device is equipped with five wavelength channels. The measurement procedure involves a quick (c. 10 s) scan of a vertical column of the atmosphere. The full specifics regarding the Microtops II sunphotometer and the Langley calibration technique used by the authors have been described in Markowicz et al. (2012), Morys et al. (2001), Strzalkowska et al. (2014), Zielinski et al. (2012).

Aerosol Optical Depth, a dimensionless, wavelength dependent parameter which refers to the reduction of the amount of direct sunlight passing through the atmosphere. It is a function of the concentration of particles, their size distribution and chemical composition. AOD values change with the change of altitude (Smirnov et al., 2009; Strzalkowska et al., 2014; Zawadzka et al., 2014; Zielinski and Zielinski, 2002). The wavelength dependence of Aerosol Optical Depth can be expressed using an empirical formula described by Ängström as follows (Carlund et al., 2005; Eck et al., 1999; Smirnov et al., 1994; Weller and Leiterer, 1988):

$$\mathrm{AOD} = \beta \times \lambda^{-\alpha}. \quad (1)$$

The β coefficient characterizes the degree of atmospheric turbidity due to aerosols and is equal to the AOD for λ = 1 μm. The Ängström Exponent (α) is dimensionless parameter allowing to estimate the aerosol size distribution and is calculated from a minimum of two wavelengths and is calculated from the following formula:

$$\alpha(\lambda_1, \lambda_2) = -\frac{\ln \mathrm{AOD}(\lambda_1) - \ln \mathrm{AOD}(\lambda_2)}{\ln\lambda_1 - \ln\lambda_2}. \quad (2)$$

During our studies, the Microtops II measurements were taken in a series of five "shots". Sets of 5 scans with the smallest standard deviation have been used in data processing. The baud rate of each instrument was set at 32, which allowed the data collection frequency to meet the NASA AERONET standards. Further improvement of the data quality involved the elimination of cloud contamination. This was achieved through a visual inspection of sky conditions during the measurements and the analyses of satellite images.

3. Results and discussion

As a result of our experiment, we obtained a set of varied AOD values. These variations were found to be correlated with the distance from the open sea. The first step in our analyses regards the meteorological situation in the studied region. Fig. 2 shows a local wind rose for (a) Ny-Ålesund station for years 1992–2013 and (b) large-scale wind rose (from NCEP/NCAR reanalysis) interpolated for the Ny-Ålesund station for years 1992–2013.

The presented wind roses show that the phenomenon of wind tunnelling along the fjord axis is the most significant process controlling local wind directions in Kongsfjorden. Local wind frequencies are qualitatively different from large-scale winds calculated in the reanalysis, concentrating along the fjord axis. Maturilli et al. (2013) conducted a

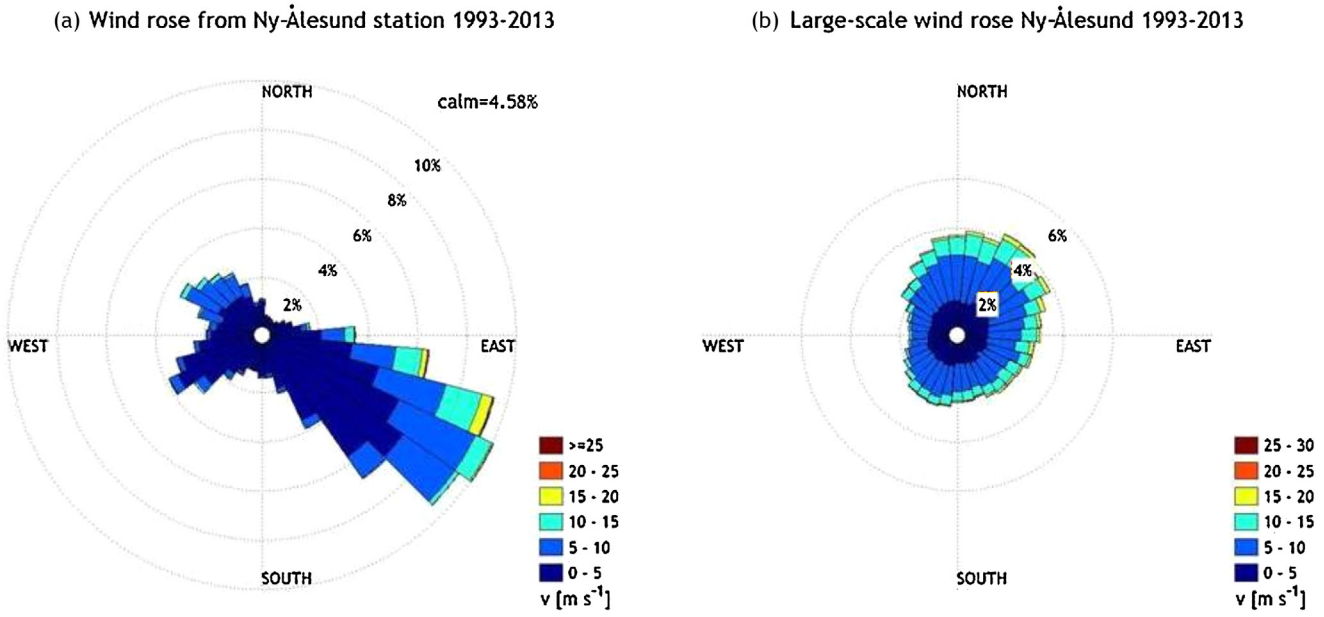

Figure 2 The local wind rose (a) and the large-scale wind rose (b) (from NCEP/NCAR reanalysis) interpolated for the Ny-Ålesund station for years 1992–2013.

Table 1 Averaged, daily wind speed and direction from measurement stations over Spitsbergen on 6 April 2014.

Station	Wind direction [°]			Average wind Speed [m s^{-1}]
	06 UTC	12 UTC	18 UTC	
Hornsund	46	87	48	3.3
Sveagruva	0	57	360	0.8
Ny-Ålesund	143	176	137	2.8
Svalbard Lufthavn	121	117	120	3.6
Pyramiden	262	285	339	2.1
Verlegenhuken	347	333	351	5.6

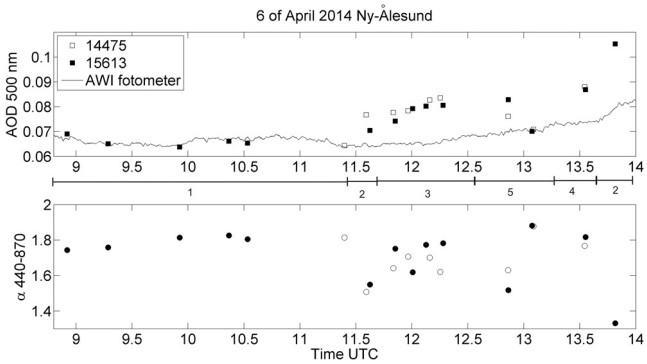

Figure 3 AOD values measured with two Microtops II sunphotometers on 6 April 2014 during the research trip in the Kongsfjorden area. The line in the middle describes consecutive measurement points, from 1 to 5.

long-term analysis of surface meteorology in Ny-Ålesund. The monthly, two-dimensional frequency distribution of wind direction presented by these authors confirms our findings, i.e. that the main wind direction in the area is from the east/south-east throughout the entire year and these conditions are very prominent in April (Maturilli et al., 2013). However, on 6 April 2014, wind situation over Spitsbergen, based on data collected from various stations, looked as presented in Table 1. Wind patterns show eastern direction component.

The results of the AOD measurements during the research trip in the area of Kongsfjorden on 6 April 2014 are presented in Fig. 3.

The measurements were taken using two Microtops II sunphotometers and they have been compared with the results from the AWI sunphotometer located at the AWI laboratory (78.92N, 11.92E). Data collection started at 8:55 UTC in Ny-Ålesund and ended at 13:43 UTC, also in Ny-Ålesund. The AOD values at the beginning of the study were low (below 0.07) for all three instruments. However, the values obtained from the AWI sunphotometer remained stable for a majority of the study period, slightly increasing (to a c. of 0.082) at the end of the study. In the case of the Microtops II measurements taken in different locations on the way to the fjord opening, the AOD values increased to a c. 0.08 close to the fjord opening, reaching the final value of 0.105 when the sunphotometers were taking measurements at the fjord opening, towards the open sea. The Ängström Exponent values remained stable during the entire study period at a level between 1.5 and 1.8, which indicates the presence of relatively small particles in the air and no advection of any other types of particles into the study area.

The spatial picture of the AOD situation on 6 April 2014 in the Svalbard region has been obtained from the NAAPS and MACC models. Fig. 4 presents the Total Optical Depth for 6 April for the entire Arctic obtained from the NAAPS model (Navy Aerosol Analysis and Prediction System, Christensen, 1997; Witek et al., 2007).

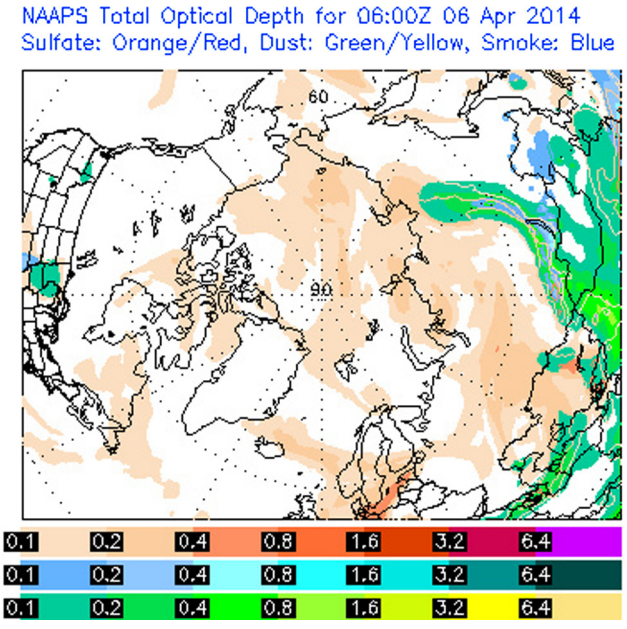

Figure 4 NAAPS derived Total Optical Depth at 06:00 on 6 April 2014 for the Arctic.

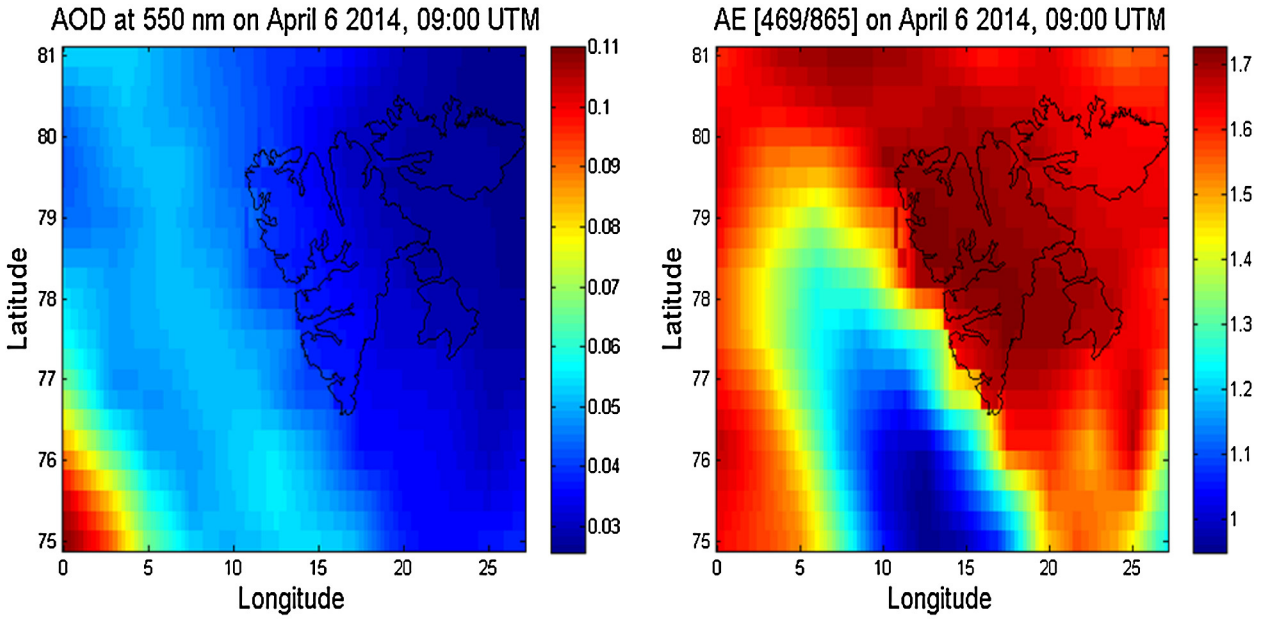

Figure 5 AOD (550 nm) and Ängström Exponent (469/865 nm) over Svalbard at 9:00 UTC on 6 April 2014 modelled using the MACC II system (http://www.gmes-atmosphere.eu).

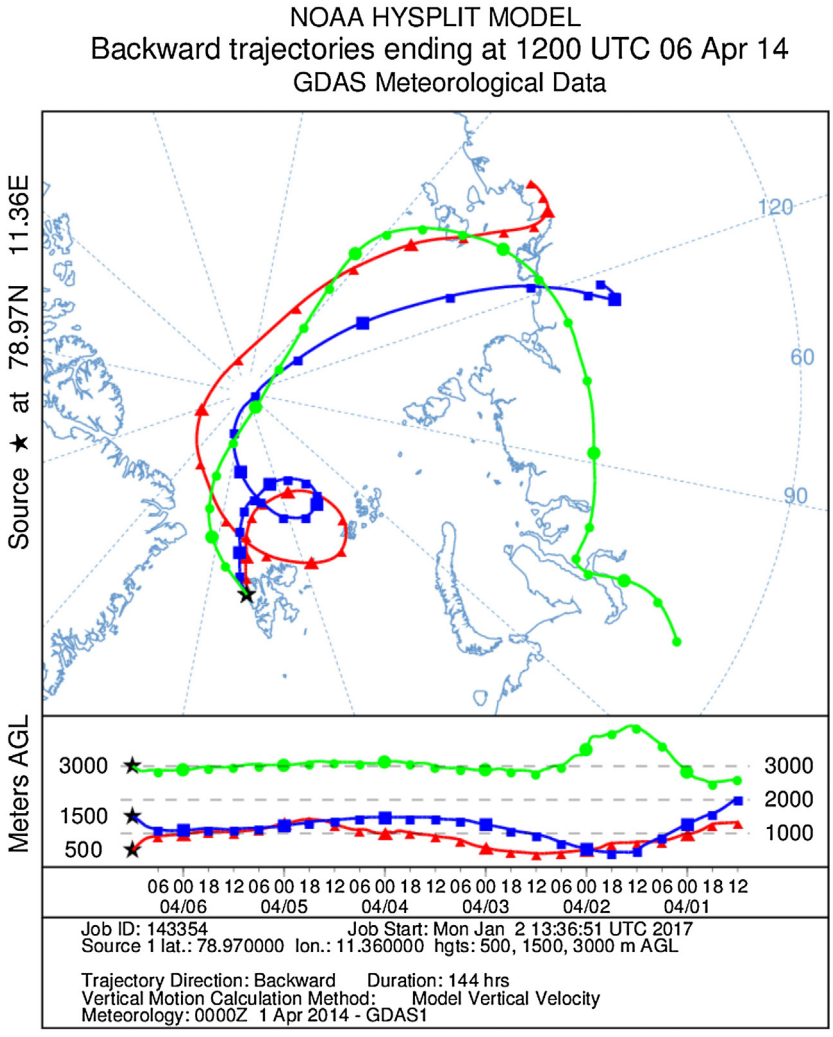

Figure 6 144-h air mass back trajectories obtained from the NOAA HYSPLIT model for 6 April 2014 at 12:00 UTC.

Fig. 4 presents the background situation of air in the Arctic and is in good agreement with the results of the sunphotometer measurements. The picture shows a slightly polluted aerosol situation over the vast area of the Arctic, including the Svalbard region. The majority of the region shows total optical depth values around 0.1 up to 0.2. Higher values (c. 0.4—0.8) are observed over Asia and at higher latitudes in Siberia, these are related to dust plumes. In the marine area of the Arctic some sulfate levels are observed which increase the optical depth to around 0.1—0.2, while off the western coast of Svalbard, these values are roughly around 0.1 and below. Even lower values have been obtained from reanalysis of AOD at 550 nm over the Svalbard region using the Monitoring Atmospheric Composition and Climate-Interim Implementation system (MACC-II) (Fig. 5).

Both graphs have been calculated for 0.25° per pixel at 9:00 UTC. Unfortunately, it is impossible to calculate these values at noon, however, all values before 9:00 UTC and at 3:00 p.m. UTC are consistent on 6 April 2014. The AOD values are in agreement with those obtained from the NAAPS model and those from the Microtops II sunphotometer measurements (Fig. 3). They range from c. 0.03 to 0.06. Additionally, the Ängström Exponent values are comparable with those from Fig. 3. They indicate the presence of mostly smaller particles in the atmosphere. It is also clear that higher values of AOD (reaching 0.07) are observed to the west of the archipelago and the values decrease eastward.

The meteorological situation over this period of time in the Svalbard region explains such a situation. Fig. 6 shows 144-h air mass back trajectories obtained from the NOAA HYSPLIT model for 6 April 2014 at 12:00 UTC.

The air mass back trajectories clearly show that on 6 April air masses were advected to the study area from over the clean Arctic region at all three altitudes above sea level. On the western side of Svalbard, they arrived in the Kongsfjorden area from over the open sea. The same pattern was observed for 4 and 5 April 2014. The NOAA obtained picture of the meteorological situation in the Svalbard region on 6 April 2014 shows wind direction at 10 m a.s.l. and air pressure changes (Fig. 7).

The situation presented in Fig. 7 indicates that the Svalbard archipelago creates a rather unique conditions in terms of wind direction patterns. In the entire region winds blew mostly from the western direction, however, over Svalbard, especially on its western side, the wind pattern was slightly different and turned from the north-west towards the north-east. This was due to a temperature difference between the cold land of the archipelago and the warm water west of the islands. This difference caused a mesoscale distortion of the pressure field in the area of the archipelago.

The observed changes in AOD relative to the distance from the open sea can be explained by greater aerosol concentration over the sea (Fig. 8).

The fact that the AOD variations had been observed at small distance changes confirms the presence of a pronounced barrier which distinguishes two air spaces with different aerosol concentrations. In our opinion, this barrier was simply a border of a breeze-like front, which was connected with convection resulting from the temperature differences between the much warmer water and colder island area. In order to verify this hypothesis, we checked if our

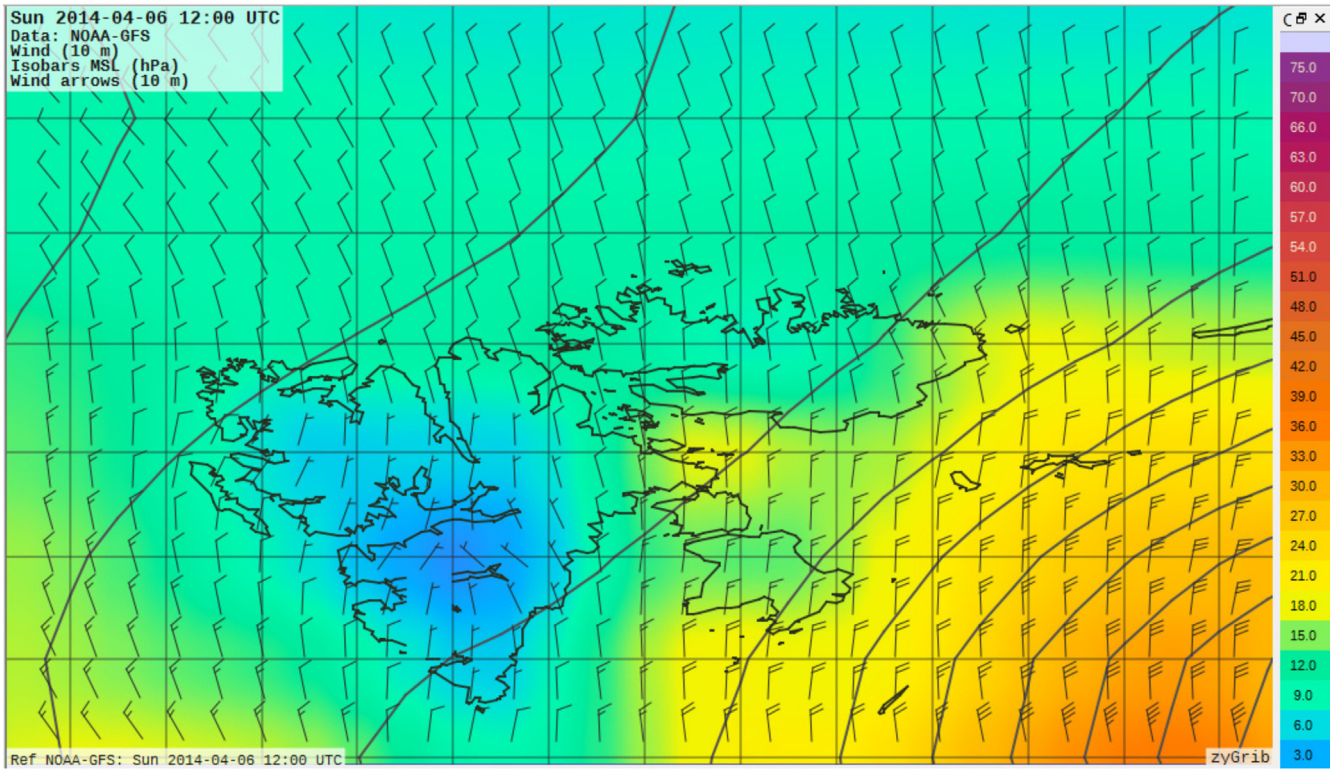

Figure 7 The NOAA — GFS generated wind direction patterns at 12:00 UTC on 6 April 2014 in the Svalbard region.

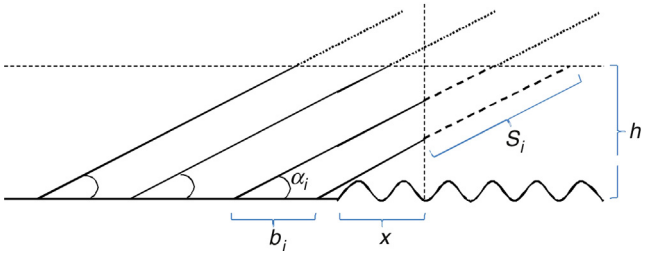

Figure 8 A conceptual picture of geometric assumptions for the result analyses. h denotes height of a breeze front a.s.l., S_i is a length of optical path through layer with higher aerosol concentration, b_i denotes distance between measurement points, while letter x denotes distance between the breeze front and the measurement point closest to the sea, and α_i denotes an angle between measurement path and surface.

results could be explained using the measurement through a layer with a higher aerosol concentration (S_i). The vertical dashed line is the breeze front and to the right (over the sea) the aerosol concentration is higher. The letters b_i denote the distance between measurement points, while the letter x denotes the distance between the breeze front and the measurement point closest to the sea. Despite the fact that we analyzed a 3D case, we decided to present the case study in this 2D form to ensure a clear presentation of the case. Calculations of the S_i distance accounted not only for angle alpha (Solar angle) but also the angles between the breeze front plane and the N–S direction (γ), and the hour angle (β_i). Therefore, the following formula was applied in our calculations:

$$S_i = \frac{h}{\sin\alpha_i} - \frac{x + b_i}{\sin(\beta_i + \gamma)\cos\alpha_i}. \quad (3)$$

During the study time, the increased wind velocity and flow structure were governed by a deep low-pressure system over the Bear Island. Fig. 9 shows vertical changes of air pressure and temperature on 6 April 2014 in Ny-Ålesund.

The radio sounding results show no atmospheric inversions up to c. 8 km a.s.l., and thus we assumed the top vertical limit in the further considerations at a level of 8 km a.s.l. Distance x was derived from the equation for S_i and we found the x value to be x = 5.7 km, which is in agreement with our estimates for the distance between the measurement point and the open sea. Following the assumption that the front plane is parallel to the western coast of the island, we assumed the γ angle to be 20°. The S_i values calculated from Eq. (3) were further correlated with the AOD values at a particular measurement point and the measurements in Ny-Ålesund. The results of such correlations are presented in Fig. 10.

This figure reveals that the AOD changes are correlated with distance S_i, at a statistically significant level, i.e. 0.613. Such a result is satisfactory since the geometry of the front, which prevented aerosol advection towards the island, has been simplified. In reality, it is not a vertical wall which does not change with time. In our opinion, these results confirm the hypothesis that the decreased levels of aerosol concentration inland, on that particular day, result from a mesoscale distortion of the pressure field, caused by a difference in temperatures between cold land and warm waters of the West Spitsbergen Current west of Svalbard.

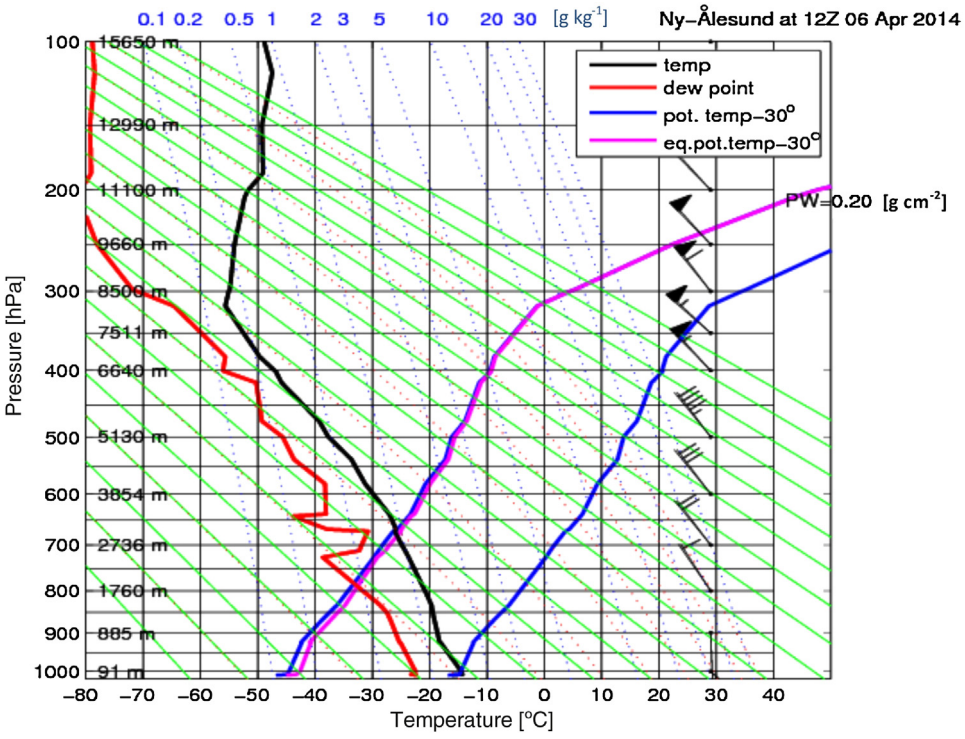

Figure 9 Vertical profile of air pressure and temperature provided by radio sounding in Ny-Ålesund at 12:00 UTC on 6 April 2014.

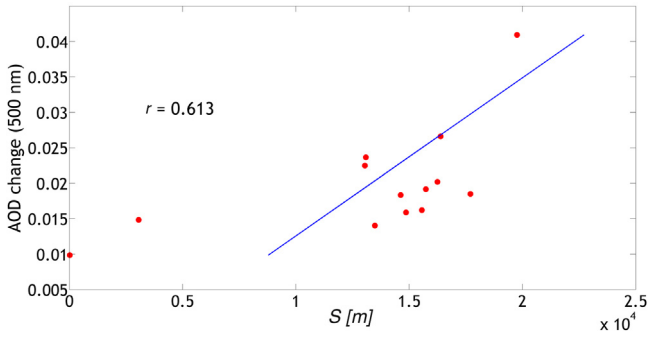

Figure 10 AOD changes versus distance during the sunphotometer study on 6 April 2014.

4. Conclusions

Firstly, these surprising changes of AOD values with the distance from the open sea in the area of Kongsfjorden are in good agreement with the model calculations. The authors are aware of the fact that the data set is not sufficient enough to provide a sound statistical analysis, thus the conclusions of the present study cannot be far-reaching. The described result is presented in a careful way. We realize that a local phenomenon of katabatic winds in one relatively small fjord cannot significantly influence AOD, or its influence is so small that it is not measurable (the impact is smaller than the measurement accuracy). This is clear from the comparison of the AOD data collected at sea level and at the Zeppelin Station (c. 450 m a.s.l). The air is so clean in the area that extinction at several 100 m a.s.l. did not show measurable values. Additionally, radio sounding results show no atmospheric inversions up to c. 8 km a.s.l. Such differences in these optical values between Ny-Ålesund and the fjord opening were most likely a result of the temperature differences between the cold archipelago and the warm waters west of the islands. These differences caused a mesoscale distortion of the pressure field in the entire archipelago area. This phenomenon should be taken into consideration while planning, and further analyzing AOD changes in this area.

Acknowledgments

The authors would like to acknowledge the support of the Polish-Norwegian Research Programme operated by the National Centre for Research and Development under the Norwegian Financial Mechanism 2009—2014 under Project Contract No. Pol-Nor/196911/38/2013 and also project KNOW, Leading National Research Centre received by the Centre for Polar Studies for the period 2014—2018 established by regulation No. 152 (2013, Nov 14) of the Rector of the University of Silesia.

This study also has been supported by funds from the GAME "Growing of Marine Arctic Ecosystem" project, funded by Narodowe Centrum Nauki grant DEC-2012/04/A/NZ8/00661.

The authors would also like to thank D. Westphal from the Naval Research Laboratory in Monterey for providing the NAAPS model input (http://www.nrlmry.navy.mil/aerosol/), and to acknowledge the MACC-II project, funded by the European Union under the 7th Framework Programme FP7 THEME [SPA.2011.1.5-02] under grant agreement no. 283576 for the provided data.

References

Argentini, S., Viola, A.P., Mastrantonio, G., Maurizi, A., Georgiadis, T., Nardino, M., 2003. Characteristics of the boundary layer at Ny-Ålesund in the Arctic during the ARTIST field experiment. Ann. Geofis. 46 (2), 185—196.

Beine, H.J., Argentini, S., Maurizi, A., Mastrantonio, G., Viola, A., 2001. The local wind field at Ny-Ålesund and the Zeppelin mountain at Svalbard. Meteorol. Atmos. Phys. 78 (1—2), 107—113.

Carlund, T., Hakansson, B., Land, P., 2005. Aerosol optical depth over the Baltic Sea derived from AERONET and SeaWiFS measurement. Int. J. Remote Sens. 26 (2), 233—245.

Christensen, J.H., 1997. The Danish Eulerian hemispheric model — a three-dimensional air pollution model used for the Arctic. Atmos. Environ. 31 (24), 4169—4191, http://dx.doi.org/10.1016/S1352-2310(97)00264-1.

Eck, T.F., Holben, B.N., Reid, J.S., Dubovik, O., Smirnov, A., O'Neill, N.T., Slutsker, I., Kinne, S., 1999. Wavelength dependence of the optical depth of biomass burning, urban, and desert dust aerosols. J. Geophys. Res. 104, http://dx.doi.org/10.1029/1999JD900923.

Engvall, A.-C., Krejci, R., Ström, J., Treffeisen, R., Scheele, R., Hermansenand, O., Paatero, J., 2008. Changes in aerosol properties during spring-summer period in the Arctic troposphere. Atmos. Chem. Phys. 8 (3), 445—462.

Esau, I., Repina, I., 2012. Wind climate in Kongsfjorden, Svalbard, and attribution of leading wind driving mechanisms through turbulence-resolving simulations. Adv. Meteorol. 568454, 16 pp, http://dx.doi.org/10.1155/2012/568454.

Førland, E.J., Hansen-Bauer, I., Nordli, P.Ø., 1997. Climate Statistics and Long-term Series of Temperature and Precipitation at Svalbard and Jan Mayen. Den Norske Meteorologiske Institutt (DNMI) Rep. 21/97 KLIMA, Oslo, Norway.

Generoso, S., Bréon, F.-M., Chevallier, F., Balkanski, Y., Schulz, M., Bey, I., 2007. Assimilation of POLDER aerosol optical thickness into the LMDz-INCA model: implications for the Arctic aerosol burden. J. Geophys. Res. 112 (D2), 2156—2202, http://dx.doi.org/10.1029/2005JD006954.

Gjelten, H.M., Nordli, O., Isaksen, K., Førland, E.J., Sviashchennikov, P.N., Wyszynski, P., Prokhorova, U.V., Przybylak, R., Ivanov, B.V., Urazgildeeva, A., 2016. Air temperature variations and gradients along the coast and fjords of western Spitsbergen. Pol. Polar Res. 38 (1), 41—60.

Hanssen-Bauer, I., Solas, M.K., Stefensen, E.L., 1990. The Climate of Spitsbergen. Den Norske Meteorologiske Institutt (DMNI) Rep. 39/90 KLIMA, Oslo, Norway.

Hartmann, J., Albers, F., Argentini, S., Bochert, A., Bonafe, U., Cohrs, W., Conidi, A., Freese, D., Georgiadis, T., Ippoliti, A., Kaleschke, L., Lüpkes, C., Maixner, U., Mastrantonio, G., Ravegnani, F., Reuter, A., Trivellone, G., Viola, A., 1999. Arctic radiation and turbulence interaction study (ARTIST). Report on Polar Research 305/1999. Alfred Wegener Institute for Polar and Marine Research, Bremerhaven, 81 pp.

Herber, A., Thomason, L.W., Gernandt, H., Leiterer, U., Nagel, D., Schulz, K.H., Kaptur, J., Albrecht, T., Notholt, J., 2002. Continuous day and night aerosol optical depth observations in the Arctic between 1991 and 1999. J. Geophys. Res. 107 (D10), 4097, http://dx.doi.org/10.1029/2001JD000536.

Hirdman, D., Burkhart, J.F., Sodemann, H., Eckhardt, S., Jefferson, A., Quinn, P.K., Sharma, S., Strom, J., Stohl, A., 2010. Long-term trends of black carbon and sulphate aerosol in the Arctic: changes in atmospheric transport and source region emissions. Atmos. Chem. Phys. 10 (19), 9351—9368, http://dx.doi.org/10.5194/acp-10-9351-2010.

Law, K.S., Stohl, A., 2007. Long-term trends of black carbon and sulphate aerosol in the Arctic: changes in atmospheric transport and source region emissions. Science 315 (5818), 1537—1540, http://dx.doi.org/10.1126/science.1137695.

Markowicz, K.M., Zielinski, T., Blindheim, S., Gausa, M., Jagodnicka, A.K., Kardas, A.E., Kumala, W., Malinowski, S., Posyniak, M., Petelski, T., Stacewicz, T., 2012. Study of vertical structure of aerosol optical properties by sun photometers and ceilometer during macron campaign in 2007. Acta Geophys. 60 (5), 1308—1337, http://dx.doi.org/10.2478/s11600-011-0056-7.

Maturilli, M., Herber, A., Konig-Langlo, G., 2013. Climatology and time series of surface meteorology in Ny-Ålesund, Svalbard. Earth Syst. Sci. Data 5 (1), 155—163, http://dx.doi.org/10.5194/essd-5-155-2013.

Maturilli, M., Herber, A., König-Langlo, G., 2015. Surface radiation climatology for Ny-Ålesund, Svalbard (78.9°N), basic observations for trend detection. Theor. Appl. Climatol. 120 (1), 331—339, http://dx.doi.org/10.1007/s00704-014-1173-4.

Mazzola, M., Stone, R.S., Herber, A., Tomasi, C., Lupi, A., Vitale, V., Lanconelli, C., Toledano, C., Cachorro, V.E., O'Neill, N.T., Shiobara, M., Aaltonen, V., Stebel, K., Zielinski, T., Petelski, T., Ortiz de Galisteo, J.P., Torres, B., Berjon, A., Goloub, P., Li, Z., Blarel, L., Abboudm, I., Cuevas, E., Stock, M., Schulz, K.-H., Virkkula, A., 2012. Evaluation of sun photometer capabilities for retrievals of aerosol optical depth at high latitudes: the POLAR-AOD intercomparison campaigns. Atmos. Environ. 52, 4—17.

Morys, M., Mims III, F.M., Hagerup, S., Anderson, S.E., Baker, A., Kia, J., Walkup, T., 2001. Design, calibration, and performance of MICROTOPS II handheld ozone monitor and Sun photometer. J. Geophys. Res.-Atmos. 106 (D13), 2156—2202.

Nicholls, N., Gruza, G.V., Jouzel, J., Karl, T.R., Ogallo, L.A., Parker, D. E., 1996. Observed climate variability and change. In: Houghton, J.T., Filho, L.G.M., Callander, B.A., Harris, N., Kattenberg, A., Maskell, K. (Eds.), Climate Change 1995: The Science of Climate Change. Cambridge Univ. Press, Cambridge, UK, 133—192.

Quinn, P.K., Shaw, G., Andrews, E., Dutton, E.G., Ruoho-Airola, T., Gong, S.L., 2007. Arctic haze: current trends and knowledge gaps. Tellus B 59 (1), 99—114.

Rozwadowska, A., Zielinski, T., Petelski, T., Sobolewski, P., 2010. Cluster analysis of the impact of air back-trajectories on aerosol optical properties at Hornsund, Spitsbergen. Atmos. Chem. Phys. 10 (3), 877—893, http://dx.doi.org/10.5194/acp-10-877-2010.

Smirnov, A., Royer, A., O'Neill, N., Tarussov, A., 1994. A study of the link between synoptic air mass type and atmospheric optical parameters. J. Geophys. Res. 99 (D10), 20967—20982.

Smirnov, A., Holben, B.N., Slutsker, I., Giles, D.M., McClain, C.R., Eck, T.F., Sakerin, S.M., Macke, A., Croot, P., Zibordi, G., Quinn, P. K., Sciare, J., Kinne, S., Harvey, M., Smyth, T.J., Piketh, S., Zielinski, T., Proshutinsky, A., Goes, J.I., Nelson, N.B., Larouche, P., Radionov, V.F., Goloub, P., Krishna Moorthy, K., Matarrese, R., Robertson, E.J., Jourdin, F., 2009. Maritime aerosol network as a component of aerosol robotic network. J. Geophys. Res. 114, 1—10, http://dx.doi.org/10.1029/2008JD011257.

Stohl, A., 2006. Characteristics of atmospheric transport into the Arctic troposphere. J. Geophys. Res.-Atmos. 111 (D11), D11306, http://dx.doi.org/10.1029/2005jd006888, 17 pp.

Stone, R.S., Sharma, S., Herber, A., Eleftheriadis, K., Nelson, D.W., 2014. A characterization of Arctic aerosols on the basis of aerosol optical depth and black carbon measurements. Elem. Sci. Anth. 2, 27, http://dx.doi.org/10.12952/journal.elementa.000027.

Strzalkowska, A., Makuch, P., Zawadzka, O., Pakszys, P., 2014. A modern approach to aerosol studies over the Baltic Sea. In: Zielinski, T., Pazdro, K., Dragan-Górska, A., Weydmann, A. (Eds.), Insights on Environmental Changes. Springer, Dordrecht, 49—64.

Tomasi, C., Kokhanovsky, A., Lupi, A., Ritter, C., Smirnov, A., O'Neill, N., Stone, R., Holben, B., Nyeki, S., Wehrli, C., Stohl, A., Mazzola, M., Lanconelli, Ch., Vitale, V., Stebel, K., Aaltonen, V., de Leeuw, G., Rodriguez, E., Herber, A.B., Radionov, V.F., Zielinski, T., Petelski, T., Sakerin, S.M., Kabanov, D.M., Xue, Y., Mei, L., Istomina, L., Wagener, R., McArthur, B., Sobolewski, P.S., Kivi, R., Courcoux, Y., Larouche, P., Broccardoz, S., Piketh, S.J., 2015. Aerosol remote sensing in polar regions. Earth-Sci. Rev. 140, 108—157.

Tomasi, C., Vitale, V., Lupi, A., Di Carmine, C., Campanelli, M., Herber, A., Treffeisen, R., Stone, R.S., Andrews, E., Sharma, S., Radionov, V., von Hoyningen-Huene, W., Stebel, K., Hansen, G.H., Myhre, C.L., Wehrli, C., Aaltonen, V., Lihavainen, H., Virkkula, A., Hillamo, R., Stroem, J., Toledano, C., Cachorro, V.E., Ortiz, P., de Frutos, A.M., Blindheim, S., Frioud, M., Gausa, M., Zielinski, T., Petelski, T., Yamanouchi, T., 2007. Aerosols in polar regions: a historical overview based on optical depth and in situ observations. J. Geophys. Res. 112 (D16), D16205, http://dx.doi.org/10.1029/2007JD008432, 28 pp.

Treffeisen, R., Herber, A., Ström, J., Shiobara, M., Yamanouchi, T., Yamagata, S., Holmén, K., Kriew, M., Schrems, O., 2011. Interpretation of Arctic aerosol properties using cluster analysis applied to observations in the Svalbard area. Tellus B 56 (5), 457—476, http://dx.doi.org/10.3402/tellusb.v56i5.16469.

Weller, M., Leiterer, V., 1988. Experimental data on spectral aerosol optical thickness and its global distribution. Beitr. Phys. Atmos. 61 (1), 1—9.

Witek, M.L., Flatau, P., Quinn, P., Westphal, D., 2007. Global sea-salt modeling: results and validation against multicampaign shipboard measurements. J. Geophys. Res. 112 (D8), D08215, http://dx.doi.org/10.1029/2006JD007779, 14 pp.

Zawadzka, O., Makuch, P., Markowicz, K.M., Zielinski, T., Petelski, T., Ulevicius, V., Strzalkowska, A., Rozwadowska, A., Gutowska, D., 2014. Studies of aerosol optical depth with use of Microtops sun photometers and MODIS detectors in the coastal areas of the Baltic Sea. Acta Geophys. 62 (2), 400—422, http://dx.doi.org/10.2478/s11600-013-0182-5.

Zielinski, T., Petelski, T., Makuch, P., Strzalkowska, A., Ponczkowska, A., Markowicz, K.M., Chourdakis, G., Georgoussis, G., Kratzer, S., 2012. Sudies of aerosols advected to coastal areas with use of remote techniques. Acta Geophys. 60 (5), 1359—1385, http://dx.doi.org/10.2478/s11600-011-0075-4.

Zielinski, T., Zielinski, A., 2002. Aerosol extinction and optical thickness in the atmosphere over the Baltic Sea determined with lidar. J. Aerosol Sci. 33 (6), 47—61.